THE ASTROPHYSICAL JOURNAL, 454:L85–L87, 1995 December 1

THE EMISSION-LINE JET IN MARKARIAN 6[1]

A. CAPETTI,[2] D. J. AXON,[2,3,4] M. KUKULA,[5] F. MACCHETTO,[2,3] A. PEDLAR,[4] W. B. SPARKS,[2] AND A. BOKSENBERG[6]
Received 1995 July 2; accepted 1995 September 11

ABSTRACT

We present the results of *Hubble Space Telescope* (*HST*) and MERLIN observations of the Seyfert 1.5 galaxy Mrk 6. FOC/*HST* images reveal a jetlike feature in the emission line which extends ~0.″5, or 250 pc, from the nucleus. The optical jet is cospatial with the southern radio jet, as revealed by a 6 cm MERLIN image matching the *HST* angular resolution, and shares with it a similar curved morphology. The emission-line jet shows a low-ionization halo surrounding a higher ionization core. This suggests that the optical jet is generated by the expansion of a halo of hot material around the radio jet.

Most of the radio and optical emission originates in the innermost 110 pc, which suggests that radio and optical emission are closely associated on this small scale.

These results strongly support the interpretation that the structure of the narrow-line region of Mrk 6, and of Seyfert galaxies with known linear radio sources, is dominated by the interaction between the radio ejecta and the surrounding medium.

Subject headings: galaxies: individual (Markarian 6) — galaxies: jets — galaxies: Seyfert

1. INTRODUCTION

It is becoming increasingly clear from *HST* studies that there is an intimate connection between the extended radio structure and that of the narrow-line region (NLR), which must result from the role interactions play in exciting and compressing the thermal gas. In objects like Mrk 573, for example (Capetti et al. 1995a), the lobelike radio features are clearly associated with concave arcs of emission whose apex lies at the position of the radio source and which suggests strongly that, as in Herbig-Haro objects, these are in fact bow shocks formed at the working surface of the advancing radio lobes. Equally convincing is the structure of the emission-line regions associated with Seyfert galaxies, which shows radio jets, e.g., Mrk 3, Mrk 348 (Capetti et al. 1995a), in which the NLR also takes the form of a linear structure that is essentially cospatial with the radio jet. This striking similarity between the morphologies, together with the kinematic structure along the length of the jets, whose hallmark is broad or split lines, implies that in reality we are seeing the cooling outer layer of a cylindrical surface that enshrouds the jet and that is expanding due to the hot gas in its interior formed by shock interaction with the jet.

Recently Kukula et al. (1995) presented spectacular new MERLIN maps of the Seyfert 1.5 galaxy Mrk 6, which not only revealed the presence of a powerful radio jet, 1″ in length, but also peculiar shell-like features that appeared to form some kind of connection between the jet and the large-scale diffuse lobes of radio emission observed with the Westerbrok Synthesis Radio telescope by Baum et al. (1993). In addition to the radio maps, Kukula et al. also carried out a ground-based study of the emission-line morphology of Mrk 6. These observations provided evidence for the existence of a large-scale radiation cone outside the jet with a morphology similar to that seen in other Seyfert 1.5 galaxies (e.g, NGC 4151, Robinson et al. 1994; NGC 3227, Mundell et al. 1995). The small angular size of the radio jet meant that with ground-based resolutions the relationship between the structure of the NLR and the radio jet could not be determined.

Here we present *HST* emission-line observations of Mrk 6 obtained with the Faint Object Camera (FOC) in the light of [O III]λ 5007 and [O II]λ 3727 together with a new high-resolution radio map, which show that there is, as with the other Seyfert galaxies discussed above, an emission-line counterpart to the radio jet of Mrk 6.

Throughout this Letter $H_0 = 50$ km s^{-1} Mpc^{-1} is adopted. Given its redshift of $z = 0.018$, Mrk 6 is at a distance of 110 Mpc, where 0.″1 corresponds to 53 pc.

2. *HST* OBSERVATIONS

Mrk 6 was observed using the FOC on board the *Hubble Space Telescope*, in the f/96, 512 × 512 mode (Nota et al. 1994); the pixel size is 0.″014 × 0.″014 and the field of view ~7″ × 7″. Images were taken using the filters F210M, F372M, F502M, and F550M. These filters isolate the oxygen lines [O III]λλ4959, 5007 and [O II]λλ3726, 3729 and the adjacent continuum. In addition, the medium-band filter F210M, centered at 2100 Å, was used to obtain a UV continuum image. The log of the observations can be found in Table 1.

The data have been reduced following the standard procedure for the FOC data (see, e.g., Capetti et al. 1995b), which includes the corrections for geometric distortion, flat-fielding and linearity, background removal, and continuum subtraction.

The flux calibration was obtained using the internal calibration of the FOC which, in this wavelength range, is accurate to within ±5%.

The images of Mrk 6 are all dominated by its nucleus, which

[1] Based on observations with the *NASA*/ESA *Hubble Space Telescope*, obtained at the Space Telescope Science Institute, which is operated by AURA, Inc., under NASA contract NAS 5-26555 and by STScI grant GO-3594.01-91A.

[2] Space Telescope Science Institute, 3700 San Martin Drive, Baltimore, MD 21218.

[3] Associated with the Astrophysics Division, Space Science Department of ESA; ESTEC, NL-2200 AG Noordwijk, The Netherlands.

[4] Nuffield Radio Astronomy Laboratories, University of Manchester, Jodrell Bank, Macclesfield, Cheshire SK11 9DL, UK.

[5] School of Chemical and Physical Sciences, Liverpool John Moores University, Byrom Street, Liverpool L3 3AF, UK.

[6] Royal Greenwich Observatory, Madingley Road, Cambridge CB3 0EZ, UK.

TABLE 1

OBSERVATION LOG

Object	Date	Root Name	Filter	Exposure Time (s)
Mrk 6.....	1994 Apr 5	X2580201T	F320W	596
		X2580202T	F372M	896
		X2580203T	F502M	750
		X2580204T	F550M	1196
		X2580205T	F210M	596
Mrk 79.....	1994 Apr 9	X2580401P	F320W	596
		X2580402P	F372M	896
		X2580403P	F502M	276
		X2580404P	F502M	618
		X2580405P	F550M	1196
		X2580406P	F210M	476

is saturated in the observations with the F372M and F502M filters (Figs. 1*a* and 1*b* [Plate L9]). The bright point source south of the nucleus is the ghost image originating in the interference filter. The contribution from the nucleus can be removed from the images by subtracting a point-spread function (PSF) template. The *HST* point-spread function is known to vary because of "breathing" of the telescope; therefore it is important to have a PSF obtained at the same epoch to accomplish such a subtraction. In addition, high signal-to-noise is required in the wings of the PSF. For these reasons, a PSF obtained with observations of a standard star is not suitable in this case. As part of this project, images of the Seyfert 1.2 galaxy Mrk 79 were also taken using the same observational procedure as for Mrk 6. The comparison of the images of Mrk 79 with a model PSF built with the Tiny Tim software (Krist 1992) show no evidence for extended emission in any image. Therefore they provide a very good representation of the PSF for the observations of Mrk 6, taken only 4 days apart, and we adopt it for our subtraction.

The residual images are shown in Figures 1*c* and 1*d*. The subtraction process is reliable only at a distance greater than 0.″2, where the effects of nonlinearity are negligible (note that the ghost completely disappears in the subtracted images).

Both the original and, more clearly, the subtracted images show a jetlike feature which extends in the southwest direction from the nucleus. A similar structure is not present in any of the continuum images (Figs. 1*e* and 1*f*). The first detected emission-line knot is located at a distance of 0.″24 from the nucleus along P.A. + 190°. The orientation of the jet beyond this location is P.A. + 220° for ∼0.″2; then it forks along P.A. + 270° and P.A. + 170° and fades below the noise level at a radius of ∼0.″5. The total projected length of the emission-line jet is ∼250 pc. The total flux of the jet outside the inner 0.″2 is $13.2 \pm 0.3 \times 10^{-14}$ ergs s^{-1} cm^{-2} and $2.7 \pm 0.2 \times 10^{-14}$ ergs s^{-1} cm^{-2} in [O III] λλ4959, 5007 and [O II] λ3727, respectively.

The [O II] emission is more diffuse than the [O III] emission. This is clearly shown by the [O III]/[O II] ratio map (Fig. 2 [Pl. L10]); the ratio between the [O III] λ5007 and [O II] λ3727 is 5–6 along the central region of the optical jet and 2–3.5 in the surrounding region.

On the north side of the nucleus there are two diffuse, low-brightness, elongated emission-line regions located at a distance of ∼0.″35 and ∼0.″6 at P.A. −45° and −75° from the nucleus, respectively. They are clearly seen in the [O III] image, while in the [O II] image, the feature closest to the nucleus is superposed to the prominent PSF spike and the second component can be only tentatively identified with a region of very low surface brightness. Their [O III] fluxes are $2.3 \pm 0.5 \times 10^{-14}$ ergs s^{-1} cm^{-2} and $3.2 \pm 0.5 \times 10^{-14}$ ergs s^{-1} cm^{-2}.

The ground-based measurement of the [O III] flux for Mrk 6 by Koski (1978) through a 2.″4 aperture is 5.0×10^{-12} ergs s^{-1} cm^{-2}. Therefore the extended components revealed by our images account for only ∼4% of the total [O III] flux. Most of the [O III] flux originates within a radius of 0.″2, 110 pc, and it is contained in the saturated region of our images; its detailed structure is therefore lost.

3. THE MERLIN OBSERVATIONS

Mrk 6 was observed with the enhanced MERLIN system (Wilkinson 1992) at 6 cm (4.997 GHz) in 1992 July. A full 18 hr track was obtained with a bandwidth of 2 × 15 MHz (30 MHz total) and a maximum baseline length of 217 km, corresponding to 3.6 Mλ.

Flux-density calibration was determined using the point source 0552+398 (DA 193) which, by comparison with 3C 286 (Baars et al. 1977), was found to have a 5 GHz flux density of 6.7 Jy. By using self-calibration solutions from the phase-reference source 0633+734 to estimate antenna gains and phase corrections for Mrk 6, the positional error in the final map was limited to ∼30 mas.

A map derived from naturally weighted data has been presented by Kukula et al. (1995). However, the resolution of this image was only 60 mas. By using a uniform weighting scheme in the standard AIPS deconvolution procedures, we have increased the angular resolution to 35 mas in order to match the *HST* images' angular resolution. Although this reduced the sensitivity slightly, reweighting of the individual MERLIN antennas resulted in an rms noise of ∼60 μJy beam^{-1}.

The resulting image in presented in Figure 3. While the northern jet linking the central radio triplet to the hot spot is completely resolved out at this resolution, this new image shows in greater detail the structure of southern jet of Mrk 6. It is dominated by a central ridge of emission that oscillates around the overall north-south orientation of the radio emission. At a distance of 0.″4 south of the central component, it widens and bends toward the west. At larger radii it extends again in the southern direction.

4. DISCUSSION

Figure 4 (Plate L11) shows the superposition of the MERLIN on the *HST* [O III] image. The registration has been performed assuming that the radio core is close to the central component of the innermost radio triplet and that this is coincident with the optical nucleus.

This comparison reveals that the emission-line jet is co-spatial with the southern radio jet. They also show a very close similarity in their small-scale structures; in particular, the wiggles in the radio jet are remarkably reproduced in the emission-line jet. Also the northern, P.A. −15°, elongated region of [O III] emission appears to be aligned with the northern radio jet, while no radio counterpart is seen for the northwestern line emission. The whole innermost triple radio structure falls within the saturated region in the *HST* image, and therefore the relation between the radio and the optical structure cannot be investigated in the innermost 110 pc.

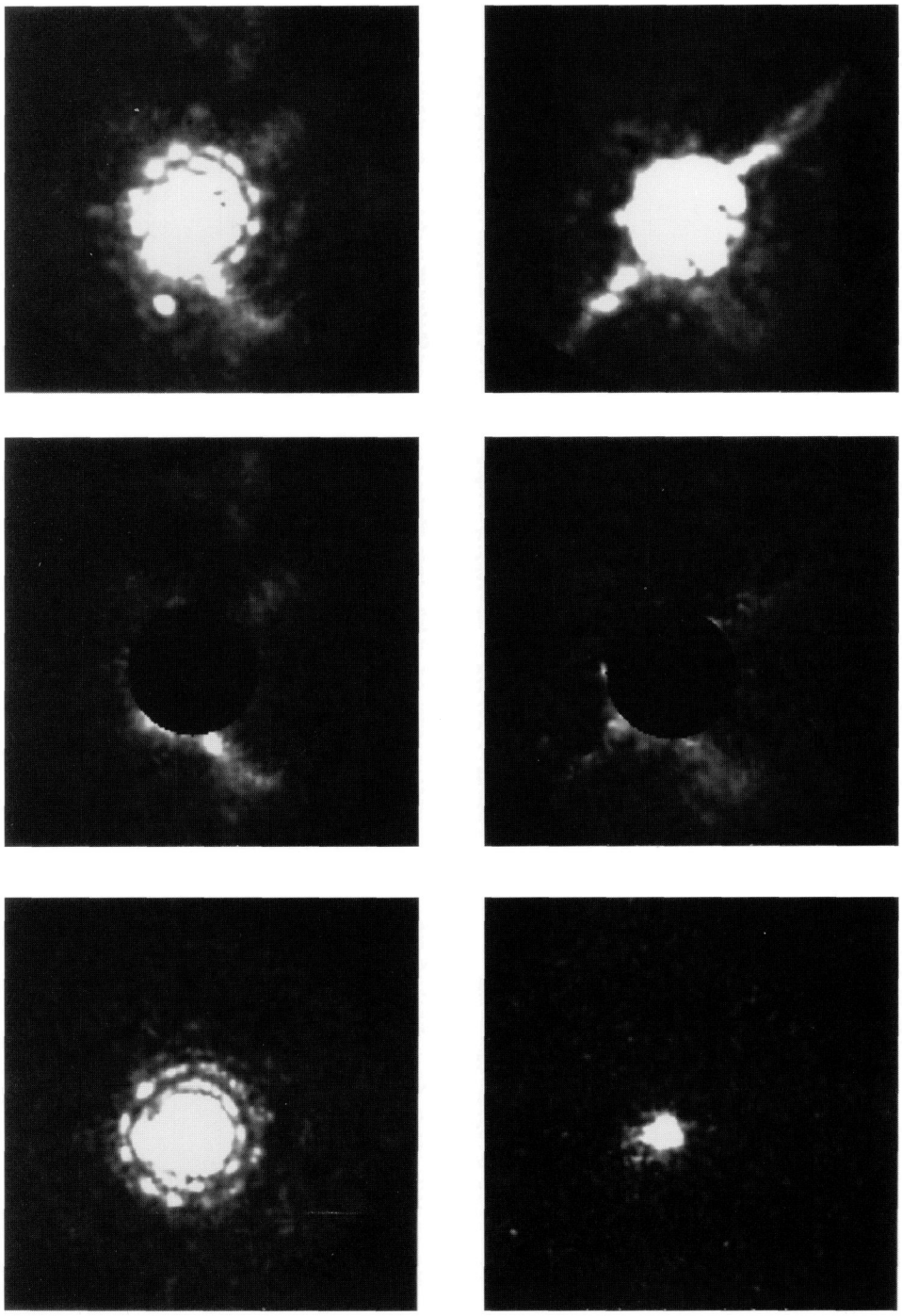

FIG. 1.—(*a*) F502M and (*b*) F372M images of Mrk 6 including the [O III] and [O II] emission lines, respectively. The bright point source south of the nucleus is the ghost image originating in the interference filter (note that it completely disappears in the subtracted images). Residual of the (*c*) F502M and (*d*) F372M images of Mrk 6 after subtraction of the nuclear point source. The black circle of radius 0.″2 masks the saturated area in these two images. (*e*) Visual and (*f*) ultraviolet continuum images of Mrk 6 taken through the F550M and F210M filters, respectively; no extended emission is detected in either continuum image. All the images in this Letter are shown with north to the top and east to the left and a field of view of 1.″4, which corresponds to 700 pc.

CAPETTI et al. (see 454, L86)

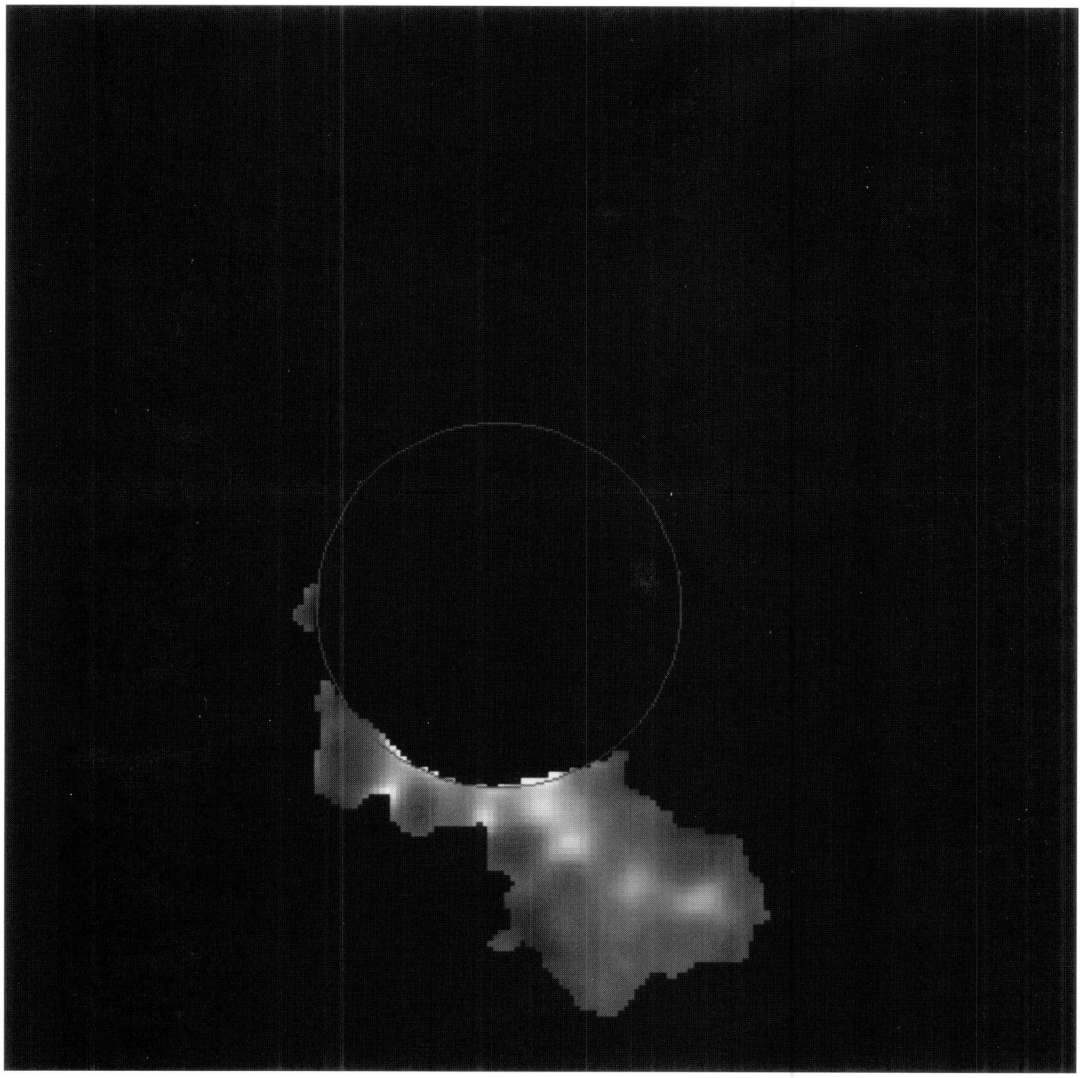

FIG. 2.—[O III]/[O II] ratio map for the optical jet of Mrk 6

CAPETTI et al. (see 454, L86)

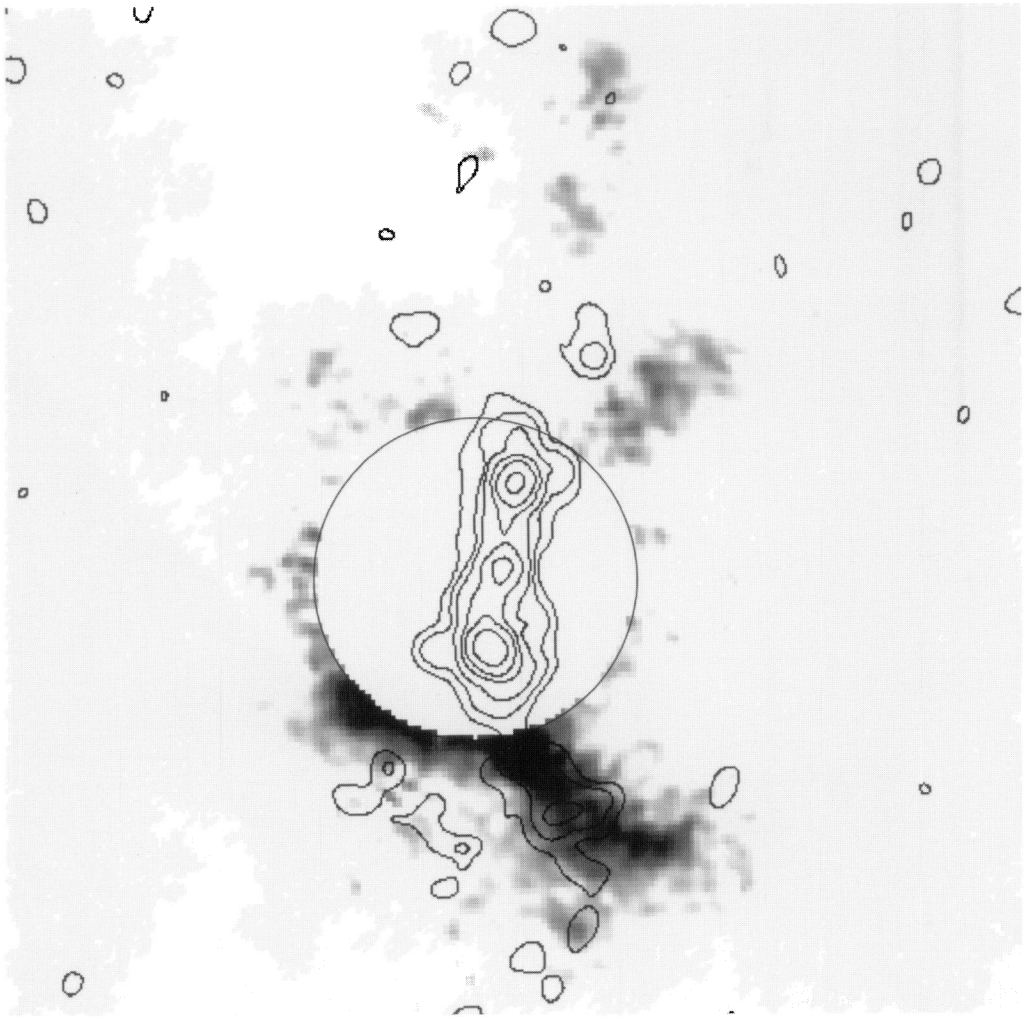

FIG. 4.—[O III] emission-line image of Mrk 6 with superposed MERLIN radio contour image. The registration has been performed assuming that the radio core is close to the central component of the innermost radio triplet and that this is coincident with the optical nucleus.

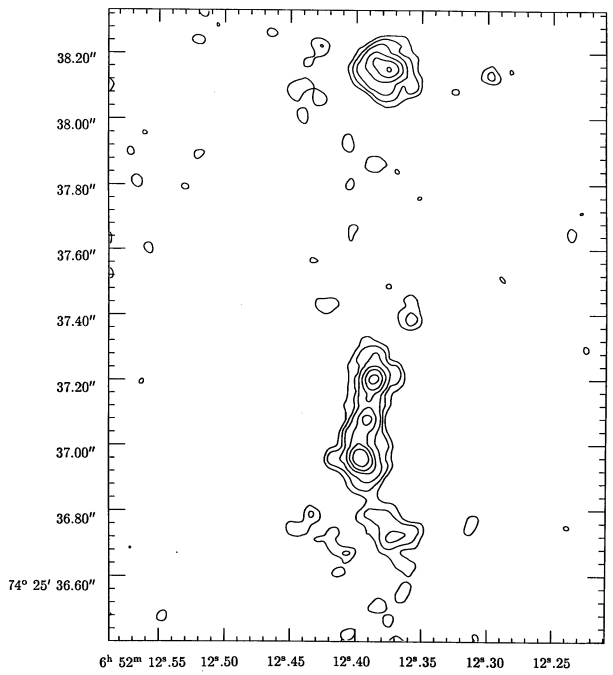

FIG. 3.—The 6 cm uniformly weighted MERLIN image. Levels are drawn at 0.01, 0.02, 0.05, 0.12, 0.25, and 0.50 times the peak value of 6.1 mJy beam^{-1}.

However, most of the line and radio emission are generated within this region.

Recently Capetti et al. (1995a, b) have shown that the radio and the emission lines are cospatial in several Seyfert 2 galaxies. In particular, in Mrk 3 and Mrk 348, which show collimated radio jets, the line emission shows a similar morphology, just as we report here in the case of Mrk 6. As in the case of Mrk 3 and Mrk 348, we suggest that the optical jet in Mrk 6 is generated by the expansion of a halo of hot interstellar material around the radio jet that is created by shocks formed by the supersonic jet as described by Taylor et al. (1992). In this picture, the line-emitting gas is stratified and its temperature decreases moving outward from the jet axis. Therefore, the gas along the radio jet has a lower density and, consequently, shows a higher ionization stage than the surrounding, denser, material just as observed in Mrk 6. Another important contribution to this effect will be local ionization from the hot gas associated with the jet itself.

Two interesting differences distinguish Mrk 6 from Mrk 3. In Mrk 3 there is no evidence of transverse ionization structure; however, a similar low-ionization halo is seen around its western radio lobe. The difference in ionization structure is unlikely due to resolution effect because the galaxies are at similar redshift and therefore it probably has a physical origin. In addition, while in Mrk 3 there is a emission-line cloud that corresponds to the radio hot spot. This is not seen on the northern hot spot of Mrk 6. One possibility is that we are seeing the jets in different phases of postshock cooling.

5. SUMMARY AND CONCLUSIONS

The *HST* images of Mrk 6 reveal a jetlike emission-line feature which extends ~0″.5, 250 pc, from its nucleus. It is observed in both oxygen emission lines; the central ridge of the jet shows a higher ionization that the surrounding diffuse emission. This optical jet is cospatial with the radio jet revealed by the MERLIN observations and shares its bent morphology.

These results strongly support the interpretation that the structure of the NLR of Mrk 6 is dominated by the compression and heating of the interstellar gas generated by shock waves formed by the supersonic radio ejecta (Pedlar et al. 1989; Taylor et al. 1992). The density stratification in the shocked gas is responsible for the inner ridge of higher ionization observed in Mrk 6.

However, the line emission originating in these regions accounts for only ~4% of the total [O III] flux of Mrk 6. Therefore most of the narrow-line emission is produced in a region smaller than 0″.25, 135 pc. Tracing the correspondence between the inner MERLIN jet and the emission-line structure would be possible with further FOC observations using neutral density filters, since the intrinsic resolution of the FOC is ~50 mas. This would be important for determining if the NLR is jetlike on this very small scale.

Only a few years ago, it was thought that jetlike radio structures in Seyfert galaxies were rare. The advent of high spatial resolution and sensitivity images, both radio and optical, is starting to show that not only the radio structure is often jetlike but also that the NLR shows a similar morphology, implying that the interaction between the thermal and nonthermal gas plays a key role in the formation of the NLR.

We thank PATT for allocation of MERLIN time. A. C. acknowledges financial support from StScI grants GO-4666 and GO-3594.

REFERENCES

Baars, J. W. M., Genzel, R., Pauliny-Toth, I. I. K., & Witzel, A. 1977, A&AS, 61, 99
Baum, S. A., O'Dea, C. P., Dallacasa, D., De Bruyn, A. G., & Pedlar, A. 1993, ApJ, 419, 553
Capetti, A., Axon, D. J., Macchetto, F., Sparks, W. B., & Boksenberg, A. 1995a, ApJ, 446, 155
Capetti, A., Macchetto, F., Axon, D. J., Sparks, W. B., & Boksenberg, A. 1995b, ApJ, L452, 87
Koski, A. T. 1978, ApJ, 223, 56
Krist, J. 1992, The Tiny Tim User's Manual, Baltimore: STScI
Kukula, M. J., Holloway, A. J., Pedlar, A., Meaburn, J., Lopez, J. A., Axon, D. J., Schilizzi, R. T., & Baum, S. A. 1995, MNRAS, in press.
Mundell, C., Holloway, A. J., Pedlar, A., Meaburn, J., Axon, D. J., Schilizzi, R. T., & Baum, S. A. 1995, MNRAS, 275, 67
Nota, A., Jedrzejewski, R., Greenfield, P., & Hack, W. 1994, Faint Object Camera Instrument Handbook, Version 5.0 (Baltimore: Space Telescope Science Inst.)
Pedlar, A., Meaburn, J., Axon, D. J., Unger, S. W., Whittle, D. M., Meurs, E. J. A., Guerrine, N., & Ward, M. J. 1989, MNRAS, 238, 863
Robinson, A., et al. 1994, A&A, 291, 473
Schilizzi, R. T., & Baum, S. A. 1995, MNRAS, submitted
Taylor, D., Dyson, J. E., & Axon, D. J. 1992, MNRAS, 255, 351
Wilkinson, P. N. 1992, in Sub-arcsecond Radio Astronomy, ed. R. J. Davis, and R. S. Booth, (Cambridge: Cambridge Univ. Press), 422